Ecosystem carbon transit versus turnover times in response to climate warming and rising atmospheric CO_2 concentration

Xingjie Lu[1,2,3], Ying-Ping Wang[3], Yiqi Luo[2,4] and Lifen Jiang[2]

[1]School of Atmospheric Sciences, Sun Yat-sen University, Guangzhou 510275, China
[2]Center for Ecosystem Science and Society, Department of Biological Sciences, Northern Arizona University, Flagstaff 86011, USA
[3]CSIRO Oceans and Atmosphere, Aspendale 3195, Australia
[4]Department for Earth System Science, Tsinghua University, Beijing 100084, China

Correspondence to: Xingjie Lu (xingjie.lu@nau.edu)

Abstract. Ecosystem carbon (C) transit time is a critical diagnostic parameter to characterize land C sequestration. This parameter has different variants in the literature, including a commonly used turnover time. However, we know little about whether transit time or turnover time better represents carbon cycling through multiple compartments under non steady state. In this study, we estimate both C turnover time as defined by the conventional stock-over-flux and mean C transit time as defined by the mean age of C mass leaving the system. We incorporate them into Community Atmosphere-Biosphere-Land Exchange model (CABLE) to estimate C turnover time and transit time, respectively, in response to climate warming and rising atmospheric $[CO_2]$. Modeling analysis shows that both C turnover time and transit time increase with climate warming but decrease with rising atmospheric $[CO_2]$. Warming increases C turnover time by 2.4 years and transit time by 11.8 years in 2100 relative to that at steady state in 1901. During the same period, rising atmospheric $[CO_2]$ decreases C turnover time by 3.8 years and transit time by 5.5 years. Our analysis shows that 65% of the increase in global mean C transit time with climate warming results from the depletion of fast-turnover C pool. The remaining 35% increase results from accompanied changes in compartment C age structures. Similarly, the decrease in mean C transit time with rising atmospheric $[CO_2]$ results approximately equally from replenishment of C into fast-turnover C pool and subsequent decrease in compartment C age structure. Greatly different from the transit time, the turnover time, which does not account for changes in either C age structure or composition of respired C, underestimated impacts of either warming or rising atmospheric $[CO_2]$ on C diagnostic time and potentially lead to biases in estimating land C sequestration in multi-compartmental ecosystems.

1 Introduction

Terrestrial ecosystem plays an important role in mitigation of climate change through sequestering carbon (C) from the atmosphere. Terrestrial C storage is co-determined by C input and C transit time, which is defined as the mean age of C mass leaving the system (Luo et al., 2001; Taylor and Lloyd, 1992; Nir and Lewis, 1975; Sierra et al., 2016; Manzoni et al., 2009; Eriksson, 1971; Bolin and Rodhe, 1973). As transit time cannot be easily estimated from observation, its variant, C turnover time, has been commonly used in the literature (Sierra et al., 2016). Recent model inter-comparison study indicated that a major cause of uncertainty in predicting future terrestrial C sequestration is the variation in C turnover time among the models (Friend et al., 2014). Up to 40% of soil C sequestration potential can be overestimated due to underestimation of C turnover time in current CMIP5 models (He et al., 2016). The C turnover time has been mostly estimated with a conventional stock-over-flux method (Carvalhais et al., 2014; Chen et al., 2013; Yan et al., 2017), which is probably first introduced by (Olson, 1963) and based on a steady-state assumption. In response to climate change, terrestrial ecosystem C dynamics move away from steady states to be at dynamic disequilibrium (Luo and Weng, 2011). Estimation of C turnover time likely deviates from C transit time in response to climate change (Sierra et al., 2016). It is not clear how much the estimate of C turnover time deviates from mean C transit time and what causes their deviation under climate change.

The C transit time as the mean age of C mass leaving the system can be estimated only from age structure of C atoms in a multi-compartment ecosystem. In contrast, the C turnover time is estimated without any information of age structure of C atoms among compartments. Thus, C turnover time is equivalent to C mean transit time only in the autonomous (i.e., time-invariant) system at steady state (Sierra et al., 2016) with two conditions to be satisfied. The first condition is that C fluxes and turnover rates of individual pools do not change with time (i.e., time invariant or autonomous). The second is that C influx to each pool equals to C efflux from the pool (i.e., at steady state). However, the autonomous and steady state conditions are usually too strict to completely meet for real-world ecosystems. For examples, ecosystem C input via photosynthesis has diurnal variation, seasonal cycle, and inter-annual variability. C turnover time also exhibits strong seasonal variation (Luo et al., 2017). With seasonal cycles and inter-annual variability in both C input and turnover time, ecosystem C cycle is rarely at steady state rather than mostly at dynamic disequilibrium (Luo and Weng, 2011). Therefore, C turnover time hardly equals C transit time in the real world, especially when land C cycle is under transient dynamics in response to climate change.

The estimates of C transit time requires information of C age structure in ecosystems so that the mean age of the C atoms at a time when they leave the system can be calculated (Manzoni et al., 2009). In a multi-compartmental ecosystem, the C age within each compartment is represented by a single compartment C mean age and different compartments have different C mean ages (Rasmussen et al., 2016). Thus, the C transit time is the weighed mean of ages of C atoms leaving different compartments according to the contributing fraction of C loss from each pool to the total C loss. In response to rising atmospheric [CO_2], increased C input with young age into an ecosystem is usually allocated more to fast than slow turnover

pools, leading to changes in the C age structure of the ecosystem. The fast turnover pools usually contribute more to the respiratory loss than the slow pools. Thus, it is expected that rising atmospheric [CO_2] decreases C transit time due to both changes in the C age structure and contributing fractions of different pools to total C loss from the ecosystem. Although it may change in response to rising atmospheric [CO_2] due to changes in both C fluxes and pools, C turnover time does not account

70   for changes in the C age structure and contributing fractions to ecosystem respiration. Consequently, estimates of C turnover time are likely to deviate from transit time estimates under climate change.

In this study, we aim to answer following questions: 1) How do both C turnover time and C transit times change in response to climate warming and rising atmospheric [CO_2]? 2) How much does the C turnover time deviate from C transit time under

75   future climate change? 3) What mechanisms cause the deviation between the two methods? 4) Which regions show the greatest biases under different climate change scenarios? To answer those questions, we incorporated new algorithm into Community Atmosphere-Biosphere-Land surface Exchange (CABLE) model (Wang et al., 2010; Wang et al., 2011) to calculate both C turnover time and transit time. We ran the modified CABLE under three climate change scenarios, climate warming only, rising atmospheric [CO2] only, and both climate warming and rising atmospheric [CO2] to compare changes in C transit time

80   with those in C turnover time.

2. Materials and Methods

2.1 The CABLE model

CABLE is a global land surface model as described by (Kowalczyk et al., 2006) and incorporates global carbon, nitrogen and phosphorus cycles (Wang et al., 2010; Wang et al., 2011). This study does not activate phosphorus cycle in the model largely

85   because phosphorus has minor impacts on C cycle (Zhang et al., 2011). Leaf photosynthesis, stomatal conductance, and heat and water transfer in CABLE are calculated using the two-leaf approach (Wang and Leuning, 1998).

Gross primary production (GPP) is calculated for both C3 and C4 plants (Farquhar et al., 1980; Kowalczyk et al., 2006). Farquhar model is a biochemical model and modified in CABLE to calculate CO_2 assimilation rate at canopy level as a

90   minimum of three potential limitation processes of photosynthesis: light, enzyme and C sink. Generally, all these three photosynthetic limitations are positively related to maximal carboxylation rate (V_{cmax}) or maximal potential electron transport rate (J_{max}) and intercellular CO_2 concentration (C_i). Both V_{cmax} and J_{max} are temperature dependent (Leuning, 2002), which are maximized at around 30°C. Thus in response to warming, model usually predicts a positive response in GPP in cold and temperate regions but a negative response in GPP in hot regions. C_i depends on the stomata conductance and atmospheric

95   [CO_2]. GPP in CABLE positively responds to rising atmospheric [CO_2]. CABLE photosynthesis is also controlled by soil moisture.

Autotrophic respiration (R_a) in CABLE is also temperature dependent, which follows modified Arrhenius formula (Ryan, 1991; Sitch et al., 2003). At the canopy scale, R_a is proportional to vegetation nitrogen content and a temperature related coefficient. R_a will positively respond to warming climate. Heterotrophic respiration (R_H) is proportional to litter and soil decomposition rate and C pool sizes. The decomposition rates in the model are controlled by soil temperature and water. The temperature response is based on a Q_{10} Eqn. Decomposition rates will positively respond to warming. The water response function is from the daily time step ecosystem model (DAYCENT) (Kelly et al., 2000) and the decomposition rate positively responds to wetter soil condition.

CABLE model has three vegetation compartments (leaf, wood and root), three litter compartments (metabolic litter, structure litter and coarse wood debris), and three soil compartments (fast soil pool, slow soil pool and passive soil pool) (Wang et al., 2010).

2.2 Simulation design

We use the meteorological data sets from National Centers for Environmental Prediction and Climatic Research Unit – (CRU-NCEP) to drive our model. The meteorological inputs from 1901 to 2100 include temperature, specific humidity, air pressure, downward solar radiation, downward long-wave radiation, rainfall, snowfall, and wind speed. The meteorological variables of CRU-NCEP data from 1901 to 2005 are interpolated from the 6-hourly into hourly (Qian et al., 2006) and re-gridded from 0.5º by 0.5º to 1.875º by 2.5º spatial resolution. From 2006 to 2100, the hourly meteorological variables are generated from Community Earth System Model version 1.0 (CESM) (Li et al., 2016; Hurrell et al., 2013) for Representative Concentration Pathway (RCP) 8.5.

C storage for all three scenarios (climate warming, rising atmospheric [CO_2] and both together) are initialized at pre-industrial steady states, which is achieved by a spin-up approach. The spin-up method cycles 10-year CRU-NCEP data (1901-1910) to drive CABLE model, with [CO_2] being constant at 1901 level. A semi-analytic solution is used to accelerate spin up simulation (Xia et al., 2012).

The description of three scenarios in this study are summarized in Table 1. Simulation one (S1) fixes the atmospheric [CO_2] but uses changing climate forcing. Simulation two (S2) fixes climate forcing but increases atmospheric [CO_2]. Simulation three (S3) uses both changing climate forcing and increasing atmospheric [CO_2].

2.3 Calculation of ecosystem C mean age

C mean age is defined as the mean time elapsed since C atoms (current in the system) entered the system, which is important for understanding C transit time described below. Following Rasmussen et al. (2016), C mean age ($\bar{a}$) can be formulated:

$$\bar{a}(t) = \frac{\sum_{i=1}^{d} a_i(t)x_i(t)}{\sum_{i=1}^{d} x_i(t)} \tag{1}$$

In Eqn (1), a_i represents the mean age of C in the ith compartment; x_i represents C pool size of the ith compartment, and d is total number of C compartments.

Mixing fresh C input into ecosystem old C may reduce the ecosystem C mean age. Meanwhile, C remaining in the system will age with the time. As shown by Rasmussen et al. (2016), dynamics of compartment C mean age can be described by the following differential equation:

$$\frac{da_i(t)}{dt} = 1 + \frac{\sum_{j=1}^{d}\left(a_j(t) - a_i(t)\right)b_{ij}k_j(t)x_j(t) - a_i(t)s_i(t)}{x_i(t)} \tag{2}$$

In Eqn (2), $s_i(t)$ is direct C input rate from net primary production to the ith compartment in g C m^{-2} year^{-1}, b_{ij} is the proportion of decomposed carbon from j^{th} compartment to be transferred to the ith compartment. k_j is the decomposition rate of the jth compartment, the unit is year^{-1}. Thus, change in compartment C age depends C aging, network C transfers among pools with different ages, and C input. Note that this equation works only for linear models.

With a time step Δt, the C transferred from the jth compartment to the ith compartment (F_{ij}) equals to $b_{ij}k_j(t)x_j(t)\Delta t$ and C input (S_i) equals to $S_i(t) = s_i(t)\Delta t$, Eqn (2) can be rewritten in a finite element form to represent C age dynamics:

$$\Delta a_i(t) = \Delta t + \frac{\sum_{j=1}^{d}\left(a_j(t) - a_i(t)\right)F_{ij} - a_i(t)S_i(t)}{x_i(t)} \tag{3}$$

In Eqn (3), the first term, Δt, indicates natural C aging. the second term, $\frac{\sum_{j=1}^{d}\left(a_j(t) - a_i(t)\right)F_{ij} - a_i(t)S_i(t)}{x_i(t)}$, represents the mean age change of the ith compartment due to mixing with transferred C from other compartments or external C input (i.e., NPP).

After the C cycle spin up, we obtain the steady state C ages in each compartment by solving Eqn (2) with an Euler method. The changes of C compartment mean age are less than 0.1% between two successive cycles.

2.4 Ecosystem C transit time

C transit time is defined as the average time for a C atom spend in the ecosystem until its exit, or the time from entering the ecosystem to leaving the ecosystem (or residence time, (Luo et al., 2001)). For a multiple-compartment system, the mean C transit time, $\bar{\tau}_R$, can be calculated using the following equation (Rasmussen et al., 2016):

$$\bar{\tau}_R(t) = \frac{\sum_{i=1}^{d} a_i(t)x_i(t)(\sum_{j=1}^{d} b_{ji})k_i(t)}{\sum_{i=1}^{d} x_i(t)(\sum_{j=1}^{d} b_{ji})k_i(t)} \tag{4}$$

When $i = j$, b_{ji} equals -1, indicating one unit of C exited from the ith compartment. When $i \neq j$, b_{ji} represents the proportion of exited C of the ith compartment transferred to j^{th} compartment. $\sum_{j=1}^{d} b_{ji} = 0$ when the exited C from the ith compartment is

fully transferred to all the other compartments, such as litterfall from plant to litter compartments, without C loss. $\sum_{j=1}^{d} b_{ji} < 0$ when the exited C from the ith compartment is partly transferred to the other compartments, such as litter or soil C decomposition, with the rest lost to the atmosphere via respiration. The denominator is the total amount of C loss from the ecosystem. The numerator is the sum of respired age-mass C.

2.5 Components of C transit time and their changes

Equation (4) can be re-organized as:

$$\bar{\tau}_R(t) = \sum_{i=1}^{d} a_i(t) f_{\text{hr},i}(t) \qquad (5)$$

when we define fraction of the total C loss from the ith compartment ($f_{\text{hr},i}$) as:

$$f_{hr,i}(t) = \frac{x_i(t)(\sum_{j=1}^{d} b_{ji}) k_i(t)}{\sum_{i=1}^{d} x_i(t)(\sum_{j=1}^{d} b_{ji}) k_i(t)}$$

Equation (5) indicates that ecosystem C transit time consists of products of two components: compartment C age (a_i) and the fractional composition of respired C ($f_{\text{hr},i}$). Compartment C age as represented by Eqn (2) changes due to C mixing with C in other compartments or external input.

According to Eqn (5), the change in ecosystem C transit time $\bar{\tau}_R$ can be attributed to the change in compartment C age (change in C age structure) and the change in respired C composition as (See Supplementary Information for details):

$$\Delta\bar{\tau}_R(t) = \sum_{i=1}^{d} a_i(t)\Delta\left(f_{\text{hr},i}(t)\right) + \sum_{i=1}^{d} f_{\text{hr},i}(t)\,\Delta\left(a_i(t)\right) + o(a_i(t), f_{\text{hr},i}(t)) \qquad (6)$$

The first term in Eqn (6) refers to C transit time change due to change in respired C composition. If the fraction of respired C from fast-turnover pool decreases, the ecosystem mean C transit time may increase because more respired C comes from slow-turnover pools with older C ages. The second term refers to C transit time change due to change in compartment C age structure. Under elevated CO_2, for example, young-age C enters a compartment more than it leaves. C in the compartment becomes younger (i.e., young-age C replenishment). Subsequently, ecosystem mean C transit time will reduce. The third term refers to residuals that cannot be explained by the previous two terms.

3. Results

3.1 Global steady-state patterns of ecosystem C transit time

The global ecosystem C transit time at steady state generally shows a latitudinal variation pattern (Fig. 1). The high values (greater than 70 years) are simulated not only in high latitude regions, such as northern Russia, northern Europe, and northern Canada but also in high altitude regions such as Tibet plateau. Small values in C transit time (less than 30 years) are simulated in tropical rainforest, such as Amazon forest, Conga forest, and Indonesia forest. Ecosystem C transit times in some grass lands in middle-south Africa, south America, Southern Great Plains of US, and central north Australia (savanna) sometime are even

smaller than that in tropical forest. The spatial patterns of the ecosystem C mean age are quite similar with the patterns of C
transit time. However, the magnitude is significantly higher than ecosystem C transit time. The ecosystem C mean age ranges
from 118 years to 7952 years, whereas ecosystem C transit time ranges only from 13 years to 341 years.

The global latitudinal pattern of C transit time in 1982-2005 is consistent with the observation-based pattern of turnover time
(Fig. 2). The latter is estimated at each grid cell globally by "stock-over-flux" method to divide ecosystem C storage by gross
primary productivity (GPP) (Carvalhais et al., 2014). The magnitude of the estimate is mostly within the uncertainty range of
the observation-based pattern. We compare estimated C transit time in 1982-2005 with the turnover time, partly to match
modelled values with contemporary observations, and partly due to the fact that terrestrial C cycle is still approximately at a
quasi-steady state between 1982 and 2005. Over the 1980s and 1990s, the annual average of global net land carbon sink
estimated from Global Carbon Project (GCP) is about 0.8 GtC yr^{-1} with an uncertainty of 0.6 GtC yr^{-1}. As a reference, the
annual average of net land carbon sink in recent decade (2007-2016) is 2.3 GtC yr^{-1} with an uncertainty of 0.7 GtC yr^{-1} (Le
Quere et al., 2018). The net change of global land carbon in 1980s and 1990s is not that significant, which indicates land C
cycle has not moved away too far from the steady state. Moreover, the simulated latitudinal pattern of C transit time almost
overlaps with C turnover time, which also evident that C cycle is still near the steady state at present day. Annual C turnover
time theoretically equals to C transit time when C cycle is close to the steady state (Sierra et al., 2016).

3.2 Responses of global C mean transit time to climate change

In 200-year simulation, global ecosystem C mean transit time increases by 11.8 years in response to climate warming (S1) and
decrease by 5.6 years in response to rising atmospheric [CO_2] (S2) (Fig. 3a). When climate warming and rising atmospheric
[CO_2] force together (S3), C transit time decreases by 1.6 years. The increase in C transit time in S1 is not significant in the
20th century but substantial in the 21st century. Oppositely, the decrease in C transit time in S2 is steady before 2060 but slow
down afterward. Mean C transit time in S3 decreases but with a smaller magnitude than that for S2 in the 21st century.

Across all the three scenarios, the majority (over 93.4%) changes in C transit time can be explained by two combined changes
in compartment C age structure and respired C composition. Changes in the compartment C age structure and the respired C
composition both significantly contribute to the total change in global C transit time. However, the contribution fraction vary
among the three scenarios at different time. In climate warming scenario (S1), respired C composition changes contribute
about 70% of the increase in C transit time in the 21st century (Fig. 3b). In the rising atmospheric [CO_2] scenario (S2), respired
C composition change and C age structure change contribute equally (Fig. 3c). When coupling climate warming and rising
atmospheric [CO_2] together in S3, respired C composition change significantly contributes only in the middle of 200-year
simulation (around year 2000), but little at the end of the 21st century. The contribution of C age structure change to the change
in C transit time gradually increases.

The increase in C transit time in climate warming scenario (S1) is the most significant from low latitude regions in South America and Africa (Fig. 4a). Respired C composition change explains most of these regional changes (Fig. 4c). The decrease in C transit time in rising atmospheric [CO2] scenario (S2) is evenly simulated all over the world (Fig. 4d). Respired C composition change also plays an important role in most regions except for North Africa with little vegetation coverage. The C transit time in combined climate warming and rising atmospheric [CO_2] scenario (S3) mostly decrease in northern hemisphere, but increase in some tropical grassland regions in South America and Africa (Fig. 4g). In those regions where C transit time decrease, compartment C age structure change due to fresh C replenishment explain most of the change in C transit time.

Note that the response under combined effects (S3) is not a sum of those from individual effects (S1 plus S2). The non-additive response to climate warming and rising atmospheric [CO_2] is probably due to their interactions, which have been commonly found in many ecological studies (Norby and Luo, 2004; Luo et al., 2008; Leuzinger et al., 2011; Campbell et al., 1997; Zhang et al., 2016).

3.3 Global C turnover time and its bias

Similar to the changes in C transit time, the global C turnover time increases with climate warming and decreases with rising atmospheric [CO_2] (Fig. 5a). However, the magnitude substantially differs between these two methods (Fig. 3a, 5a). In response to climate warming (S1), global ecosystem C turnover time increases by only 2.4 year at end of the simulation, which is only one-fifth of the increase in C transit time (11.8 year). In response to rising atmospheric [CO_2] (S2), global C turnover time decreases by 3.7 year, whereas C transit time decreases by 5.6 year. In response to the coupled scenario (S3) where climate warming and rising atmospheric [CO_2] force together, global ecosystem C turnover time decreases by 4.5 year, while C transit time decreases by only 1.6 year.

In 1901, the global C turnover time is about 0.5 year longer than the C transit time (Fig. 3a, Fig. 5a). Theoretically, C turnover time equals transit time when land C cycle is at steady state. The offset at the initial state of simulations probably results from C seasonal cycles, which is not at steady state. The underestimates of the change in C turnover time relative to C transit time increases in climate warming scenario (S1) by up to 9.4 years in the end of the 21st century, which is 79.6% of the total increase in C transit time (Fig. 5b). In rising atmospheric [CO_2] scenario (S2), the bias constantly grows to about 1.9 years, a 27.7% of the underestimated decrease in C turnover time. In climate warming and rising atmospheric [CO_2] scenario (S3), the change in C turnover time is overestimated by 2.9 years or 181.1% in relative to the change in C transit time in 2100 (Fig. 5b, 5c).

3.4 Latitudinal variation in C turnover time and its bias

Latitudinal patterns in C transit time and C turnover time at the initial state in 1900 are nearly the same. Steady state estimates are both from 20 years in low latitude to 100 years in high latitude (Fig. 6a, 6d). However, significant bias still exists in high latitudes (north of 60^oN and south of 50^oS) (Fig. 6g), because seasonal soil frozen-thaw processes in this region lead to the strong seasonal cycle of the soil decomposition and violate the steady state assumption of the C turnover time. The underestimates of C turnover time can be up to 10 years in high latitude regions, which is about 8% of C transit time. In other area, bias of turnover time is less than 0.5 years.

Changes in C turnover time and C transit time deviate in different regions in response to climate warming (S1) (Fig. 6b, 6c, 6e, 6f). In temperate and tropical regions, C transit time significantly increases, while C turnover time also increases but in a much smaller magnitude. In tropics, C transit time increases by 13 years in 2100, up to 60% of the initial value in 1900, whereas C turnover time increase by only 2 years. In the high latitude region, C transit time slightly decreases (Fig. 6b and c) but C turnover time significantly decreases by several decades in the high latitude (Fig. 6f). In some regions between 40^oN and 60^oN, C transit time increases but turnover time decreases in response to climate warming. C turnover time overall changes less than C transit time in the S1 scenario. Warming-induced changes in C turnover time is underestimated by 5% at the high latitude of the southern hemisphere to 50% at the low latitude (Fig. 6h), which range from 2 to 29 years (Fig. 6i).

In response to rising atmospheric [CO_2] (S2), both C turnover time and transit time decrease. The magnitude of changes for both of them are generally greater at the mid latitudes than those at either low or high latitudes (Fig. 6b, 6e). At most latitudes, C turnover time decreases less than C transit time, leading to the positive bias (Fig. 6h and 6i). The deviation of the change is higher in the low than high latitude. In response to rising atmospheric [CO_2], the underestimate of the decrease in C turnover time is by at most 2 years in absolute bias or 10% in relative bias (Fig. 6h, 6i).

In climate warming and rising atmospheric [CO_2] scenario (S3), C turnover time and C transit time decrease at most of the latitudinal regions except for some tropic areas (Fig. 6b, 6c, 6e, 6f). The decrease in C turnover time is more than that in C transit time (Fig. 6h, 6i). Especially in high latitudes, the difference in changes is much more significant. C turnover time is reduced by up to three decades (Fig. 6f) or 35% (Fig. 6e), whereas C transit time shows nearly no relative changes in those. Bias in these areas can be up to 27 years (Fig. 6i).

4. Discussion

4.1 C transit time and its two components

Changes in C transit time can be explained by its two components: the respired C composition and compartment C age structure. The first component is to account for different contributions of respired C from different pools to total ecosystem C loss. Previous studies have demonstrated that pathways of respiring C from multiple compartments are variably controlled by global change factor (Luo et al., 2001). Results from this study provide more spatial details about where C transit time change due to respired C composition change. For example, over 80% of the increase in C transit time under warming is explained by respired C composition change in the South America grassland region (Fig. 4a). In contrast, change in respired C composition only accounts for approximately 10% of the increase in C transit time under warming in the boreal and high latitude region of North America.

The second component is the C age structure, primarily from change in C mean age of individual pool modified by relative fraction of each pool. In coupled climate warming with rising atmospheric $[CO_2]$ scenario (S3), C age structure change primarily contributes to the C transit time response in most global regions in 2100 (Fig. 4h). In this scenario, ecosystem mean C transit time decreases by 1.6 years. The decrease in C transit time results from increased young-age C uptake with rising atmospheric $[CO_2]$, which is more than the increased young-age C loss with warming. A previous study has also shown that models with multiple pools usually have a more heterogeneous C age structure and thus can store extremely older C than a single pool model (Manzoni et al., 2009).

4.2 Bias arising from estimated C turnover time

C turnover time has been widely used to quantify ecosystem C cycle partly because both ecosystem C storage and C flux can be easily measured (Sanderman et al., 2003; Chen et al., 2013; Carvalhais et al., 2014; McCulley et al., 2004; Raich and Schlesinger, 1992; Yan et al., 2017). The C turnover time has been theoretically shown to equal C transit time at steady state but they deviate under non-steady states (Sierra et al., 2016). This study illustrates how much deviation occurs between C transit time and C turnover time in response to three scenarios of climate change. Our results show that even at initial steady state, global ecosystem C turnover time is slightly greater than C transit time by 3%. This is because the steady state reached by spin-up does not mean the terrestrial C cycle system is completely at equilibrium. Seasonal variations of ecosystem C uptake and turnover still lead to periodical oscillation of the terrestrial C cycle.

The deviation between C transit time and turnover time also indicates to what extend that turnover time can properly represent time characteristics in C cycle. In climate warming and rising atmospheric $[CO_2]$ scenario (S3), the deviation does not increase significantly until 2050. The modeled latitudinal pattern of present-day C transit time well matches the C turnover time estimated from observations (Carvalhais et al., 2014). It indicates that the stock-over-flux estimates are still useful at present

day. However, the deviation between C transit time and turnover time remarkably increases after 2050 (Fig 5b). Then, it requires caution when we use the C turnover time for estimating C sequestration in multiple compartmental ecosystems.

310

In transient state, the changes in C transit time and C turnover time differ the most in climate warming scenario (S1). Tropical and high latitude regions contribute the most of the deviation (Fig. 6h, 6i). In tropical and subtropical regions, C transit time increases by about 60% (Fig. 6b) while C turnover time increases by 20% or less (Fig. 6e). The great difference between changes in C transit time and turnover time is due to their different assumptions. In response to climate warming, composition
315 change in respired C contributes most to the change in C transit time in tropical regions. However, C turnover time assumes the whole ecosystem C as one homogenous pool, even if both plant and soil C can be extremely heterogeneous. This homogeneity assumption ignores the composition changes in respired C, which causes up to 80% of change in C transit time.

In high latitude regions, C transit time slightly decreases by up to 10%, whereas C turnover time considerably decreases by
320 over 30% in response to climate warming. Warming significantly increases soil respiration due to permafrost thaw, whereas the change in permafrost ecosystem C pool size is relatively small. Thus, C turnover time significantly decreases. C transit time slowly responds to climate warming because the young-age C input added to permafrost ecosystem is relatively small compared to large C storage in this area and C age structure does not change much. These big deviations between C turnover time and C transit time in tropical and permafrost regions suggest that future C cycle analysis based on turnover time likely
325 leads to strong biases as it does not represent transient C dynamics in multi-pool ecosystems.

4.3 C transit time versus turnover time under other global change scenarios

This study has illustrated how C transit time and turnover time deviate under climate warming and rising atmospheric [CO_2] scenarios. Those deviations may become even bigger under other global change scenarios. For example, land use change and fire can drive ecosystems out of steady state to be at disequilibrium (Luo and Weng, 2011). Clearcut of forest or forest fire
330 removes at least the aboveground wood C pools and thus greatly changes both the total C stock and NPP, leading to a large change in C turnover time (Wang et al., 1999; Zhou and Luo, 2008). Clearcut of forest or forest fire also changes age structure and composition of respired C from different pools within the ecosystem, resulting in change in C transit time. Such a disturbance usually drives ecosystem to a stronger degree of disequilibrium than climate change does. The deviation between turnover time and transit time should be bigger under a severe disturbance than climate change, since our results have indicated
335 that C transit time and turnover time deviates more significantly when an ecosystem is further away from equilibrium (Fig. 5).

In contrast to the static vegetation distribution used in CABLE, natural vegetation distribution may change over time in the real world. C transit time and turnover time may further deviate under natural vegetation dynamics. However, whether forest will expand or dieback in a future warming world is still quite unknown. Previous studies variously conclude due to their focus
340 on different areas with different methods (Masek, 2001; Soja et al., 2007; Cox et al., 2004; Cox et al., 2013). Nevertheless,

most bioclimatic models consistently suggest temperate and boreal biomes rapidly increase in area under warming (Kirilenko and Solomon, 1998). If the forest species, which stores more C in slow-turnover tissue, takes over the grass species, which stores more C in fast-turnover tissue, the expansion of forest may increase C transit time significantly. However, C turnover time by lumping all different C compartments together may underestimate such changes.

345

In the real world, land C cycle is always at dynamic disequilibrium due to cyclic environmental conditions (e.g., diurnal, seasonal, and interannual variability), directional global change (e.g., climate warming, rising atmospheric CO_2 concentration, altered precipitation, and nitrogen deposition), recursive disturbance-recovery cycles, shifted climatic and disturbance regimes, and vegetation changes (Luo and Weng, 2011). Thus, the estimated C turnover time is expected to differ from the C transit

350 time at any time point and at any spatial location. The degree of deviation between C turnover time and transit time may vary.

In addition to various agents to cause ecosystem to be at disequilibrium, deviation between estimated C transit time and turnover time also depends on model structure. Vertically resolved soil C models, for example, includes vertical C mixing and depth-dependent C decomposition rates (Koven et al., 2013; Huang et al., 2018). Representation of vertically resolved

355 processes likely increase soil heterogeneity. When warming induces deep soil thaw and increases deep soil decomposition, the fraction of respired C from deep layer with old-age C increases. The C transit time together with a vertically resolved model may substantially increase whereas C turnover time, which implicitly assumes ecosystem as one homogeneous pool, may not respond much.

4.4 Estimation of C transit time in the real world

360 Previous studies have argued that C transit time is conceptually sounder than C turnover time (Rasmussen et al., 2016; Sierra et al., 2016). In this study, we have shown that the C turnover time can substantially deviate from the transit time in response to climate change and other environmental change. However, C turnover time can be easily calculated from C stock over flux, both of which can be easily measured. In contrast, C transit time cannot be easily estimated from field measurements. Equation (5) indicates that we need data from measurement of C mean ages (a_i) and fractional composition of respired C ($f_{hr,i}$) in

365 individual C pools in order to calculate ecosystem mean C transit time ($\bar{\tau}_R$). Neither a_i nor $f_{hr,i}$ can be easily measured in field. Thus, our research community faces a tremendous challenge to estimate a conceptually sound and scientifically important parameter.

In the past, radiocarbon ^{14}C has been used to quantify C mean ages of various litter and soil pools (Gaudinski et al., 2000).

370 Measured soil respiration in response to elevated CO_2 treatment in Duke Forest has been decomposed to various fractional composition using a deconvolution method or inverse analysis (Luo et al., 2001). It appears that estimation of C transit time in the real-world ecosystems requires measurement of isotope signatures in different litter and soil fractions together with measurement of respiration from soil surface and soil components. Those measurements, together with many other data sets,

may need to be analyzed to estimate C mean ages, fractional composition of respired C in individual C pools, and then

375   ecosystem mean C transit time ($\bar{\tau}_R$) using some innovative ways, such as data assimilation.

Estimating C transit times in the real world can help constrain projections in land C sequestration by C cycle models because C turnover time is a major source of model uncertainty (Friend et al., 2014; He et al., 2016). Our study has shown that the change in C transit time can be separated into two components, C composition change and C age change. Assessment on the

380   two components would provide additional constraints on model projections. To further constrain C transit time through its two components with observation, modelled C cycle and land C sequestration can be significantly improved.

5. Conclusions

This study explores how global ecosystem C transit time deviates from the turnover time under climate warming and rising

385   atmospheric [CO_2]. Although both global ecosystem C transit time and turnover time increase in response to climate warming and decrease in response to rising atmospheric [CO_2], their deviations increase with time in all the three climate change scenarios. In 2100, the deviations are high in tropical regions under climate warming scenario (S1) and rising atmospheric [CO_2] scenario (S2), and in high latitude regions under S1 and combined change scenario (S3). Knowledge about the deviation between C transit time and turnover time in different regions under different scenarios (warming and [CO_2] rising) is useful

390   for us to understand time characteristic of the ecosystem carbon dynamics. When we lump all pools and fluxes together to calculate turnover time by "stock over flux", the time characteristic is different from that of transit time when individual pools and fluxes are considered within a networked compartmental system. Thus, our results provide information on how turnover time in the future could deviates from transit time in specific regions and natural ecosystems under different climate change scenarios.

395

The changes in C transit time results from both the C age structure changes and composition changes in respired C in multi-pool ecosystems. The C age structure changes mainly depend on young-age C replenishment from external C input. The composition change is due to differential responses of various C pools to climate warming and rising atmospheric [CO_2]. However, C turnover time assumes ecosystem as one homogeneous pool, and it does not account for changes in age structure

400   and contribution fractions of different pools to ecosystem respiration. Thus, C transit time is a better parameter than C turnover time to characterize C cycle in multi-pool ecosystems, especially when they are at transient states.

However, C transit time cannot be easily measured because it requires information of the C age structure and composition of respired C. Both of them are usually not measurable in field studies. Radiocarbon ^{14}C measurement in the field has the potential

405   to offer information on mean C ages in various pools. It is not easy, either, to estimate contribution fractions of different pools

from measured ecosystem or soil respiration to respired C. We may have to combine compartment models with different types of measurements via data assimilation techniques to estimate both age structure and composition of respired C before we can estimate ecosystem C transit time.

410 **Acknowledgments**

This research was financially supported by the post-doctoral fellowship from the CSIRO Office of Chief Executive to X.J.L and U.S. Department of Energy grants DE-SC0008270, DE-SC0014085, and U.S. National Science Foundation (NSF) grants EF-1807529 and OIA-1301789 to Y.Q.L EcoLab.

415

References

Bolin, B., and Rodhe, H.: A note on Concepts of Age Distribution and Transit-Time in Natural Reservoirs, Tellus, 25, 58-62, 1973.
Campbell, B. D., Stafford Smith, D. M., and McKeon, G. M.: Elevated CO2 and water supply interactions in grasslands: A pastures and rangelands management perspective, Global Change Biol, 3, 177-187, 1997.
420 Carvalhais, N., Forkel, M., Khomik, M., Bellarby, J., Jung, M., Migliavacca, M., Mu, M. Q., Saatchi, S., Santoro, M., Thurner, M., Weber, U., Ahrens, B., Beer, C., Cescatti, A., Randerson, J. T., and Reichstein, M.: Global covariation of carbon turnover times with climate in terrestrial ecosystems, Nature, 514, 213-+, 10.1038/nature13731, 2014.
Chen, S. T., Huang, Y., Zou, J. W., and Shi, Y. S.: Mean residence time of global topsoil organic carbon depends on temperature, precipitation and soil nitrogen, Global Planet Change, 100, 99-108, 2013.
425 Cox, P. M., Betts, R. A., Collins, M., Harris, P. P., Huntingford, C., and Jones, C. D.: Amazonian forest dieback under climate-carbon cycle projections for the 21st century, Theor Appl Climatol, 78, 137-156, 2004.
Cox, P. M., Pearson, D., Booth, B. B., Friedlingstein, P., Huntingford, C., Jones, C. D., and Luke, C. M.: Sensitivity of tropical carbon to climate change constrained by carbon dioxide variability, Nature, 494, 341-344, 10.1038/nature11882, 2013.
Eriksson, E.: Compartment models and reservoir, Annual Review of Ecology and Systematics, 2, 67-84, 1971.
430 Farquhar, G. D., Caemmerer, S. V., and Berry, J. A.: A Biochemical-Model of Photosynthetic Co2 Assimilation in Leaves of C-3 Species, Planta, 149, 78-90, Doi 10.1007/Bf00386231, 1980.
Friend, A. D., Lucht, W., Rademacher, T. T., Keribin, R., Betts, R., Cadule, P., Ciais, P., Clark, D. B., Dankers, R., Falloon, P. D., Ito, A., Kahana, R., Kleidon, A., Lomas, M. R., Nishina, K., Ostberg, S., Pavlick, R., Peylin, P., Schaphoff, S., Vuichard, N., Warszawski, L., Wiltshire, A., and Woodward, F. I.: Carbon residence time dominates uncertainty in terrestrial vegetation responses to future climate and 435 atmospheric CO2, P Natl Acad Sci USA, 111, 3280-3285, 10.1073/pnas.1222477110, 2014.
Gaudinski, J. B., Trumbore, S. E., Davidson, E. A., and Zheng, S. H.: Soil carbon cycling in a temperate forest: radiocarbon-based estimates of residence times, sequestration rates and partitioning of fluxes, Biogeochemistry, 51, 33-69, 2000.
He, Y. J., Trumbore, S. E., Torn, M. S., Harden, J. W., Vaughn, L. J. S., Allison, S. D., and Randerson, J. T.: Radiocarbon constraints imply reduced carbon uptake by soils during the 21st century, Science, 353, 1419-1424, 10.1126/science.aad4273, 2016.
440 Huang, Y. Y., Lu, X. J., Shi, Z., Lawrence, D., Koven, C. D., Xia, J. Y., Du, Z. G., Kluzek, E., and Luo, Y. Q.: Matrix approach to land carbon cycle modeling: A case study with the Community Land Model, Global Change Biol, 24, 1394-1404, 2018.
Hurrell, J. W., Holland, M. M., Gent, P. R., Ghan, S., Kay, J. E., Kushner, P. J., Lamarque, J. F., Large, W. G., Lawrence, D., Lindsay, K., Lipscomb, W. H., Long, M. C., Mahowald, N., Marsh, D. R., Neale, R. B., Rasch, P., Vavrus, S., Vertenstein, M., Bader, D., Collins, W. D., Hack, J. J., Kiehl, J., and Marshall, S.: The Community Earth System Model A Framework for Collaborative Research, B Am Meteorol 445 Soc, 94, 1339-1360, 10.1175/Bams-D-12-00121.1, 2013.
Kelly, R. H., Parton, W. J., Hartman, M. D., Stretch, L. K., Ojima, D. S., and Schimel, D. S.: Intra-annual and interannual variability of ecosystem processes in shortgrass steppe, J Geophys Res-Atmos, 105, 20093-20100, Doi 10.1029/2000jd900259, 2000.
Kirilenko, A. P., and Solomon, A. M.: Modeling dynamic vegetation response to rapid climate change using bioclimatic classification, Climatic Change, 38, 15-49, 1998.
450 Koven, C. D., Riley, W. J., Subin, Z. M., Tang, J. Y., Torn, M. S., Collins, W. D., Bonan, G. B., Lawrence, D. M., and Swenson, S. C.: The effect of vertically resolved soil biogeochemistry and alternate soil C and N models on C dynamics of CLM4, Biogeosciences, 10, 7109-7131, 10.5194/bg-10-7109-2013, 2013.
Le Quere, C., Andrew, R. M., Friedlingstein, P., Sitch, S., Pongratz, J., Manning, A. C., Korsbakken, J. I., Peters, G. P., Canadell, J. G., Jackson, R. B., Boden, T. A., Tans, P. P., Andrews, O. D., Arora, V. K., Bakker, D. C. E., Barbero, L., Becker, M., Betts, R. A., Bopp, L.,

455 Chevallier, F., Chini, L. P., Ciais, P., Cosca, C. E., Cross, J., Currie, K., Gasser, T., Harris, I., Hauck, J., Haverd, V., Houghton, R. A., Hunt, C. W., Hurtt, G., Ilyina, T., Jain, A. K., Kato, E., Kautz, M., Keeling, R. F., Goldewijk, K. K., Kortzinger, A., Landschutzer, P., Lefevre, N., Lenton, A., Lienert, S., Lima, I., Lombardozzi, D., Metzl, N., Millero, F., Monteiro, P. M. S., Munro, D. R., Nabel, J. E. M. S., Nakaoka, S., Nojiri, Y., Padin, X. A., Peregon, A., Pfeil, B., Pierrot, D., Poulter, B., Rehder, G., Reimer, J., Rodenbeck, C., Schwinger, J., Seferian, R., Skjelvan, I., Stocker, B. D., Tian, H. Q., Tilbrook, B., Tubiello, F. N., van der Laan-Luijkx, I. T., van der Werf, G. R., van Heuven, S.,
460 Viovy, N., Vuichard, N., Walker, A. P., Watson, A. J., Wiltshire, A. J., Zaehle, S., and Zhu, D.: Global Carbon Budget 2017, Earth Syst Sci Data, 10, 405-448, 2018.

Leuning, R.: Temperature dependence of two parameters in a photosynthesis model, Plant Cell Environ, 25, 1205-1210, DOI 10.1046/j.1365-3040.2002.00898.x, 2002.

Leuzinger, S., Luo, Y. Q., Beier, C., Dieleman, W., Vicca, S., and Korner, C.: Do global change experiments overestimate impacts on
465 terrestrial ecosystems?, Trends Ecol Evol, 26, 236-241, 2011.

Li, J. D., Wang, Y. P., Duan, Q. Y., Lu, X. J., Pak, B., Wiltshire, A., Robertson, E., and Ziehn, T.: Quantification and attribution of errors in the simulated annual gross primary production and latent heat fluxes by two global land surface models, J Adv Model Earth Sy, 8, 1270-1288, 10.1002/2015ms000583, 2016.

Luo, Y., and Weng, E.: Dynamic disequilibrium of the terrestrial carbon cycle under global change, Trends Ecol Evol, 26, 96-104,
470 10.1016/j.tree.2010.11.003, 2011.

Luo, Y. Q., Wu, L. H., Andrews, J. A., White, L., Matamala, R., Schafer, K. V. R., and Schlesinger, W. H.: Elevated CO2 differentiates ecosystem carbon processes: Deconvolution analysis of Duke Forest FACE data, Ecological Monographs, 71, 357-376, 10.1890/0012-9615(2001)071[0357:Ecdecp]2.0.Co;2, 2001.

Luo, Y. Q., Gerten, D., Le Maire, G., Parton, W. J., Weng, E. S., Zhou, X. H., Keough, C., Beier, C., Ciais, P., Cramer, W., Dukes, J. S.,
475 Emmett, B., Hanson, P. J., Knapp, A., Linder, S., Nepstad, D., and Rustad, L.: Modeled interactive effects of precipitation, temperature, and [CO2] on ecosystem carbon and water dynamics in different climatic zones, Global Change Biol, 14, 1986-1999, 2008.

Luo, Y. Q., Shi, Z., Lu, X. J., Xia, J. Y., Liang, J. Y., Jiang, J., Wang, Y., Smith, M. J., Jiang, L. F., Ahlstrom, A., Chen, B., Hararuk, O., Hastings, A., Hoffman, F., Medlyn, B., Niu, S. L., Rasmussen, M., Todd-Brown, K., and Wang, Y. P.: Transient dynamics of terrestrial carbon storage: mathematical foundation and its applications, Biogeosciences, 14, 145-161, 10.5194/bg-14-145-2017, 2017.

480 Manzoni, S., Katul, G. G., and Porporato, A.: Analysis of soil carbon transit times and age distributions using network theories, J Geophys Res-Biogeo, 114, Artn G04025
10.1029/2009jg001070, 2009.

Masek, J. G.: Stability of boreal forest stands during recent climate change: evidence from Landsat satellite imagery, J Biogeogr, 28, 967-976, 2001.

485 McCulley, R. L., Archer, S. R., Boutton, T. W., Hons, F. M., and Zuberer, D. A.: Soil respiration and nutrient cycling in wooded communities developing in grassland, Ecology, 85, 2804-2817, Doi 10.1890/03-0645, 2004.

Nir, A., and Lewis, S.: Tracer Theory in Geophysical Systems in Steady and Non-Steady State .1., Tellus, 27, 372-383, 1975.

Norby, R. J., and Luo, Y. Q.: Evaluating ecosystem responses to rising atmospheric CO(2) and global warming in a multi-factor world, New Phytol, 162, 281-293, 2004.

490 Olson, J. S.: Energy-Storage and Balance of Producers and Decomposers in Ecological-Systems, Ecology, 44, 322-&, Doi 10.2307/1932179, 1963.

Qian, T. T., Dai, A., Trenberth, K. E., and Oleson, K. W.: Simulation of global land surface conditions from 1948 to 2004. Part I: Forcing data and evaluations, J Hydrometeorol, 7, 953-975, Doi 10.1175/Jhm540.1, 2006.

Raich, J. W., and Schlesinger, W. H.: The Global Carbon-Dioxide Flux in Soil Respiration and Its Relationship to Vegetation and Climate,
495 Tellus B, 44, 81-99, DOI 10.1034/j.1600-0889.1992.t01-1-00001.x, 1992.

Rasmussen, M., Hastings, A., Smith, M. J., Agusto, F. B., Chen-Charpentier, B. M., Hoffman, F. M., Jiang, J., Todd-Brown, K. E. O., Wang, Y., Wang, Y. P., and Luo, Y. Q.: Transit times and mean ages for nonautonomous and autonomous compartment systems, J Math Biol, 73, 1379-1398, 2016.

Ryan, M. G.: Effects of Climate Change on Plant Respiration, Ecol Appl, 1, 157-167, Doi 10.2307/1941808, 1991.

500 Sanderman, J., Amundson, R. G., and Baldocchi, D. D.: Application of eddy covariance measurements to the temperature dependence of soil organic matter mean residence time, Global Biogeochem Cy, 17, Artn 1061
10.1029/2001gb001833, 2003.

Sierra, C. A., Muller, M., Metzler, H., Manzoni, S., and Trumbore, S. E.: The muddle of ages, turnover, transit, and residence times in the carbon cycle, Glob Chang Biol, 10.1111/gcb.13556, 2016.

505 Sitch, S., Smith, B., Prentice, I. C., Arneth, A., Bondeau, A., Cramer, W., Kaplan, J. O., Levis, S., Lucht, W., Sykes, M. T., Thonicke, K., and Venevsky, S.: Evaluation of ecosystem dynamics, plant geography and terrestrial carbon cycling in the LPJ dynamic global vegetation model, Global Change Biol, 9, 161-185, DOI 10.1046/j.1365-2486.2003.00569.x, 2003.

Soja, A. J., Tchebakova, N. M., French, N. H. F., Flannigan, M. D., Shugart, H. H., Stocks, B. J., Sukhinin, A. I., Parfenova, E. I., Chapin, F. S., and Stackhouse, P. W.: Climate-induced boreal forest change: Predictions versus current observations, Global Planet Change, 56, 274-
510 296, 2007.

Taylor, J. A., and Lloyd, J.: Sources and Sinks of Atmospheric CO2, Aust J Bot, 40, 407-418, Doi 10.1071/Bt9920407, 1992.

Trumbore, S.: Age of soil organic matter and soil respiration: Radiocarbon constraints on belowground C dynamics, Ecol Appl, 10, 399-411, 2000.

Wang, Y., Amundson, R., and Trumbore, S.: The impact of land use change on C turnover in soils, Global Biogeochem Cy, 13, 47-57, 1999.

515   Wang, Y. P., and Leuning, R.: A two-leaf model for canopy conductance, photosynthesis and partitioning of available energy I: Model description and comparison with a multi-layered model, Agr Forest Meteorol, 91, 89-111, Doi 10.1016/S0168-1923(98)00061-6, 1998.

Wang, Y. P., Law, R. M., and Pak, B.: A global model of carbon, nitrogen and phosphorus cycles for the terrestrial biosphere, Biogeosciences, 7, 2261-2282, DOI 10.5194/bg-7-2261-2010, 2010.

Wang, Y. P., Kowalczyk, E., Leuning, R., Abramowitz, G., Raupach, M. R., Pak, B., van Gorsel, E., and Luhar, A.: Diagnosing errors in a
520   land surface model (CABLE) in the time and frequency domains, Journal of Geophysical Research-Biogeosciences, 116, 2011.

Xia, J. Y., Luo, Y. Q., Wang, Y. P., Weng, E. S., and Hararuk, O.: A semi-analytical solution to accelerate spin-up of a coupled carbon and nitrogen land model to steady state, Geosci Model Dev, 5, 1259-1271, 10.5194/gmd-5-1259-2012, 2012.

Yan, Y., Zhou, X. H., Jiang, L. F., and Luo, Y. Q.: Effects of carbon turnover time on terrestrial ecosystem carbon storage, Biogeosciences, 14, 5441-5454, 2017.

525   Zhang, Q., Wang, Y. P., Pitman, A. J., and Dai, Y. J.: Limitations of nitrogen and phosphorous on the terrestrial carbon uptake in the 20th century, Geophys Res Lett, 38, 2011.

Zhang, X. Z., Rayner, P. J., Wang, Y. P., Silver, J. D., Lu, X. J., Pak, B., and Zheng, X. G.: Linear and nonlinear effects of dominant drivers on the trends in global and regional land carbon uptake: 1959 to 2013, Geophys Res Lett, 43, 1607-1614, 2016.

Zhou, T., and Luo, Y. Q.: Spatial patterns of ecosystem carbon residence time and NPP-driven carbon uptake in the conterminous United
530   States, Global Biogeochem Cy, 22, 10.1029/2007gb002939, 2008.

Table 1 Summary of scenarios and forcing data.

Scenario name	Simulation abbreviation	Climate forcing	CO_2 data
Climate warming scenario	S1	Climate warming[#]	Pre-industrial[**]
CO_2 direct effect scenario	S2	Pre-industrial[##]	CO_2 increase[*]
Full effect scenario	S3	Climate warming[#]	CO_2 increase[*]

[#] Climate warming forcing data from 1901 to 2005 uses CRU-NCEP dataset. The forcing data from 2006 to 2100 uses CESM output under Representative Concentration Pathways with radiative forcing increased by 8.5 W m^{-2} (RCP8.5).

[##] Pre-industrial climate forcing repeatedly uses one-year climatology data averaged over 1901 to 1910 from CRU-NCEP
535   dataset.

[*] CO_2 concentration data are from 200-year CMIP5 dataset under historical and future scenario (RCP8.5).

[**] Pre-industrial CO_2 concentration is from CMIP5 dataset for the year 1901.
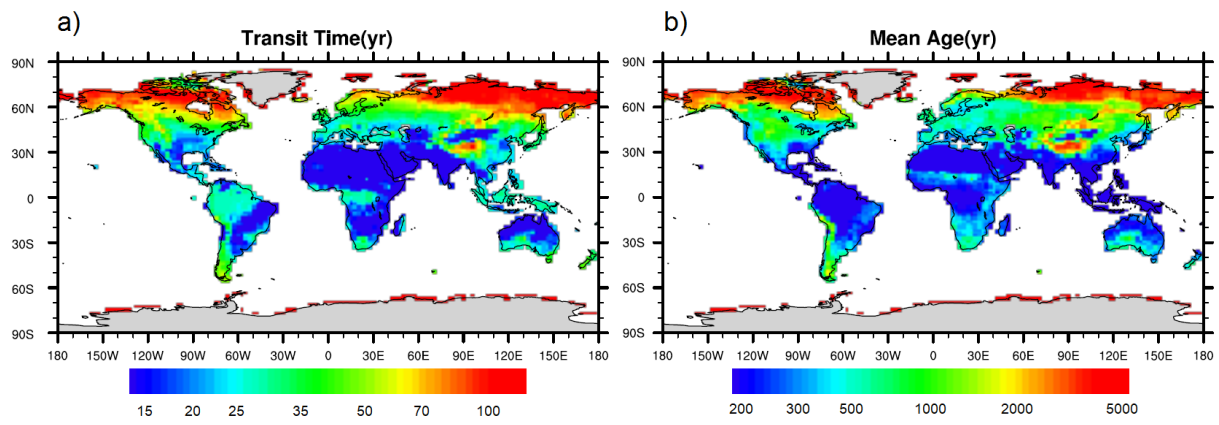
540   **Figure 1 Global maps of a) carbon transit time and b) carbon mean age are the average over 1901 to 1910 at each grid cell.**
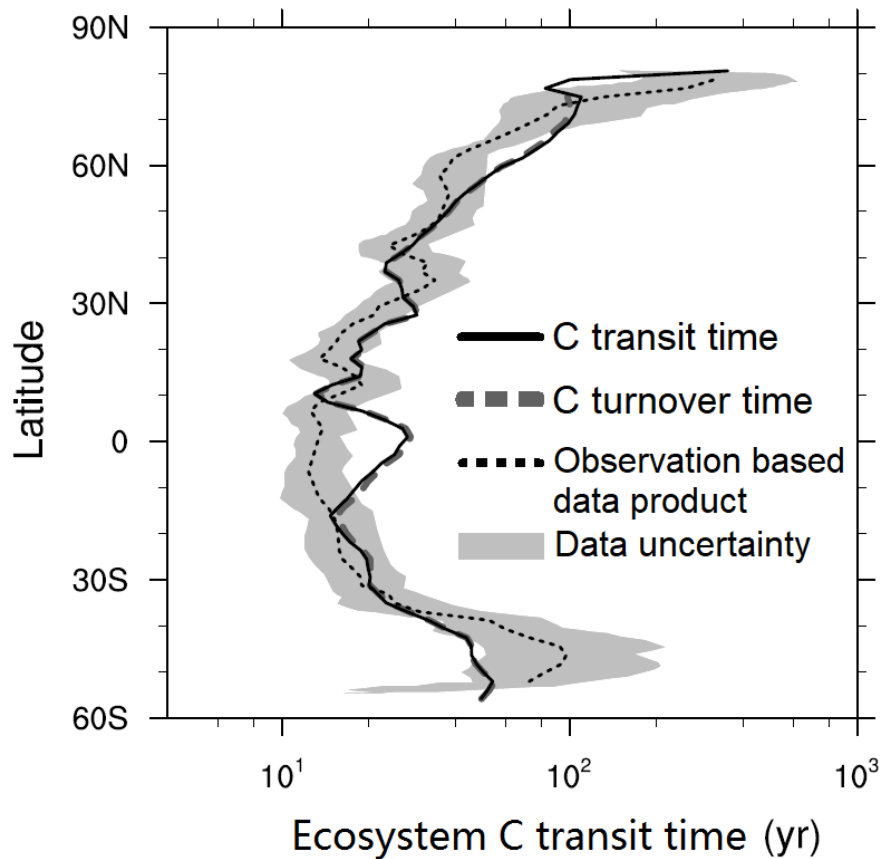
Figure 2 Validation of simulated latitudinal variation pattern in ecosystem C transit time. Comparison of the ecosystem C mean transit time from 1982 to 2005 as estimated in this study with the estimates from observation (Carvalhais et al., 2014) and simulated C turnover time from CABLE. Grey area indicates the uncertainty range of observation-based data. Our assumption, which is also used by some other ecological studies (Trumbore, 2000), is that present-day ecosystem C cycle is closed to the steady state. Especially, in 1980s and 1990s, global land C uptake from Global Carbon Project (GCP) is about 0.8 GtC yr^{-1} with an uncertainty of 0.6 GtC yr^{-1}, which is not significant compared to current decade with global land C uptake is 2.7 GtC yr^{-1}. (Le Quere et al., 2018)

550
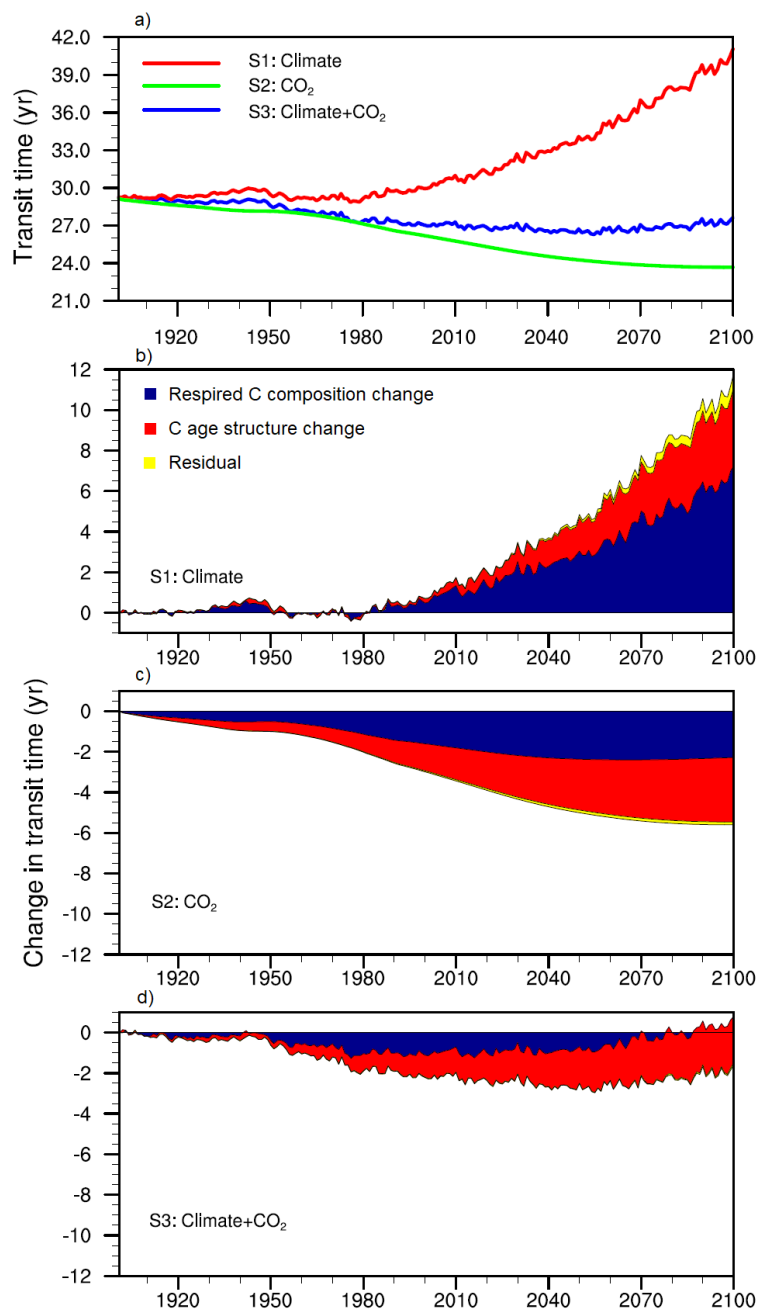
Figure 3 CABLE simulates changes of global C transit time for each of the three scenarios in a): S1: climate warming scenario (red line); S2: rising atmospheric [CO₂] scenario (green line), and S3: Combining climate warming and rising atmospheric [CO₂] scenario (blue line). The changes in global ecosystem C transit time are separated into three contributions based on Equation (6): contribution from respired C composition change, contribution from C age structure change and residual (b-d).

555
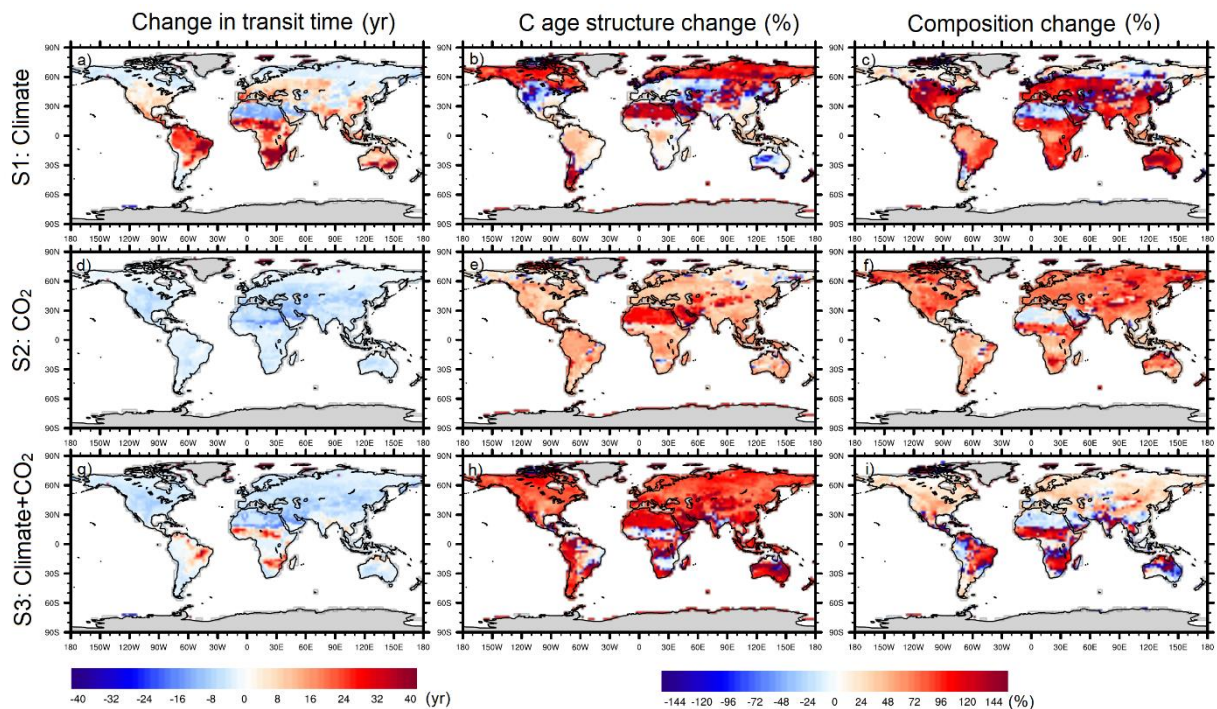
Figure 4 Global map of the change in C transit time in three scenarios, a) S1: climate warming scenario; d) S2: rising atmospheric [CO2] scenario, and g) S3: Combination of climate warming and rising atmospheric [CO2] scenario. In these three scenarios, contribution from C age structure change and contribution from respired C composition change are also estimated in relative to the change in C transit time (S1: b) and c); S2: e) and f); S3: h) and i)). The calculation of contribution from C age structure change and

560 **contribution from respired C contribution change are based on Equation (6). The positive contribution indicates the C age structure change or composition change leads to C transit time change towards the same direction.**
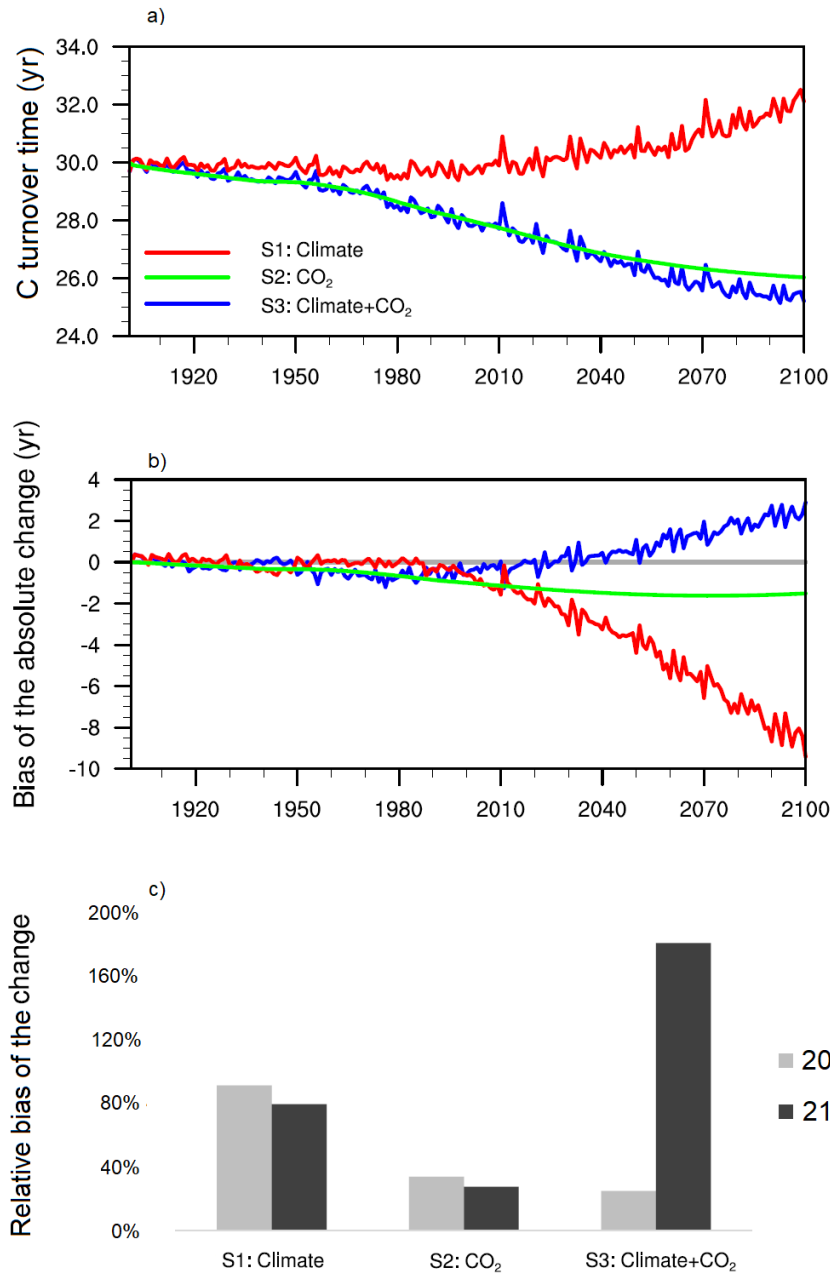
Figure 5 a) Changes of global C turnover time (stock-over-flux) in three scenarios, S1: climate warming scenario (red line); S2: rising atmospheric [CO₂] scenario (green line), and S3: Combination of climate warming and rising atmospheric [CO₂] scenario (blue line). b) The bias of the change in C turnover time ($\Delta\tau_o$) is estimated relative to the change in C transit time ($\Delta\tau_R$): ($|\Delta\tau_o| - |\Delta\tau_R|$). Positive indicates more change in C turnover time than C transit time. Grey line represents the reference of no bias. c) The relative bias of the change in C turnover time in year 2000 and 2100 is also estimated relative to the change in C transit time: $\frac{(|\Delta\tau_o| - |\Delta\tau_R|)}{|\Delta\tau_R|} \times 100\%$.

570
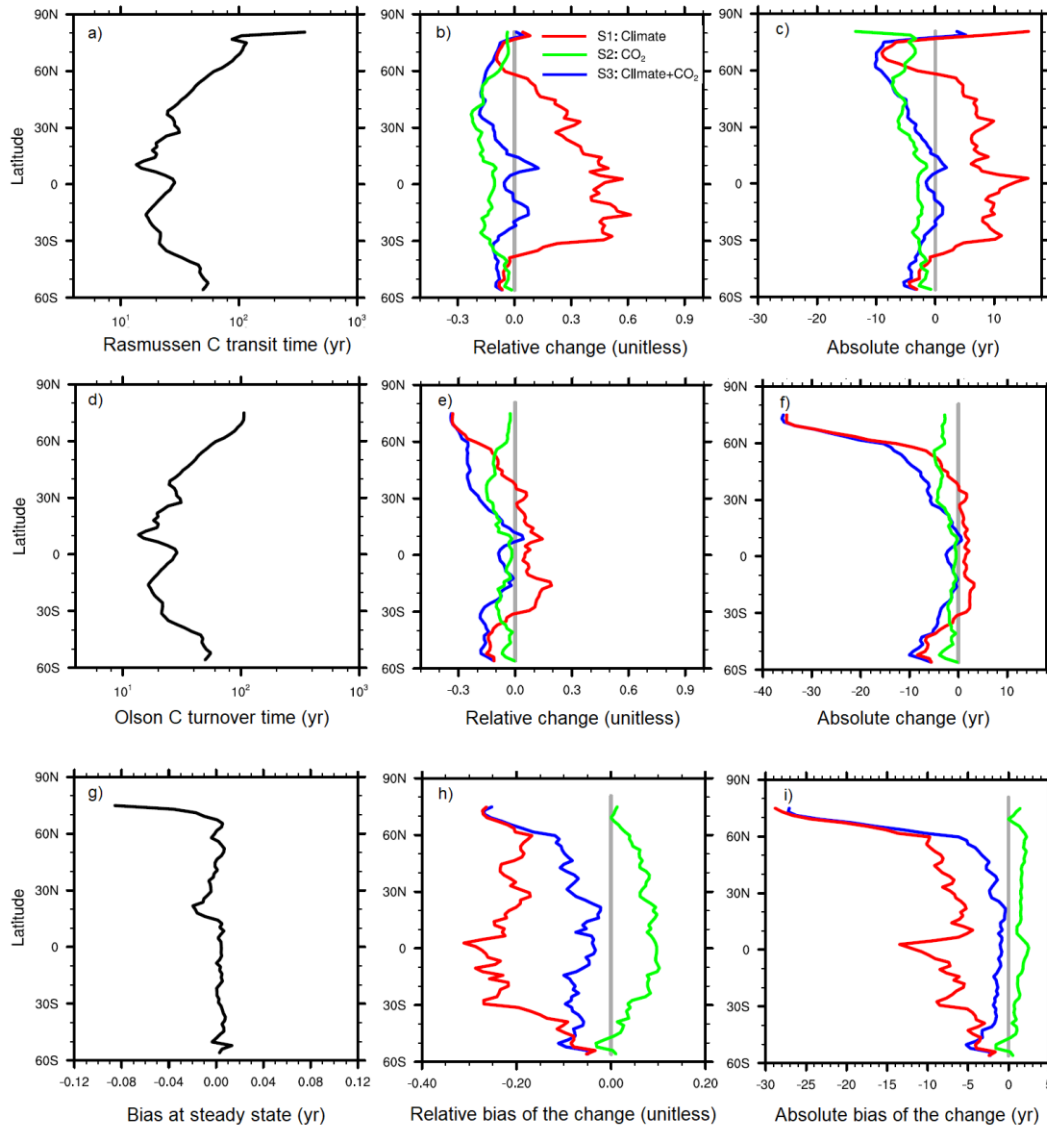
Figure 6 a) Latitudinal variation in C transit time (τ_R) at steady state and b)-c) its change are compared to d)-f) C turnover time (τ_o). The changes between 2090s and 1900s are estimated by c), f) absolute value: $\Delta\tau = (\tau_{2090s} - \tau_{1900s})$ and by b), e) relative value: $\Delta\tau_r = \frac{\Delta\tau}{\tau_{1900s}}$. g) The bias of C turnover time in relative to C transit time is estimated by $(\tau_o - \tau_R)$ at steady state. In relative to C transit time, the bias of the change in C turnover time are estimated by h) absolute bias $(|\Delta\tau_o| - |\Delta\tau_R|)$ and i) relative bias in

575 $\frac{(|\Delta\tau_o| - |\Delta\tau_R|)}{|\Delta\tau_R|}$. **All variables are compared in three scenarios: S1: only climate warming scenario (red line); S2: rising atmospheric [CO₂] scenario (green line), and S3: Combination of climate warming and rising atmospheric [CO₂] scenario (blue line). Grey lines in b), c), e) and f) represent the reference lines of no change and those in h) and i) represent reference line of no bias.**